

Measuring Laser Wavelength with Filtered-Photodiode Color Sensors

Tyler B Jones

A senior thesis submitted to the faculty of  
Brigham Young University  
in partial fulfillment of the requirements for the degree of  
Bachelor of Science

Dallin S Durfee, Advisor

Department of Physics and Astronomy

Brigham Young University

April 2015

Copyright © 2015 Tyler B Jones

All Rights Reserved

## ABSTRACT

### Measuring Laser Wavelength with Filtered-Photodiode Color Sensors

Tyler B Jones

Department of Physics and Astronomy, BYU

Bachelor of Science

One type of color sensor made for consumer electronics uses an array of optically filtered photodiodes. The filters cause the photodiodes' measurements to depend on the wavelength and the intensity of the incident light. The relative amounts of light measured by each photodiode can then be used to determine the light's color. These sensors are made for use with broadband light, but the data sheet for one such sensor, the TCS3414, lists very few limitations on its capabilities, indicating that the sensor may be useful in laser spectroscopy. This document explores the TCS3414's performance in laser spectroscopy. Considerations such as algorithmic method, intensity, bit noise, and temperature dependence will be discussed. Measurements show that the sensor's measurements are repeatable and accurate to within less than 10 picometers for time scales on the order of a day. While this is not precise enough to directly find atomic transitions, it is precise enough to get the laser close enough to the transition that it can then be scanned to find the transition without mode hopping. It is also comparable to many mid-grade interferometers. Therefore, the sensor is viable as an alternative method for measuring laser wavelength for short time scales.

Keywords: laser wavelength, color sensor, photodiode, measurement

## ACKNOWLEDGMENTS

I would like to thank all those who have been influential on the progress of this research. First, I would like to thank Nils Otterstrom, whose work was conducted in tandem with mine. The ideas for the current algorithm, calibration, that the temperature variance originated from an etalon, and some of the circuitry design were his. The current version of the software used to interface with the sensors, the bit noise computation, and the Bland-Altman diagram were my work. We worked together to develop the Allan deviation. I would also like to thank James Archibald, Kevin Blisset, and Jarom Jackson, whose ideas helped shape the project, and Dr. Dallin Durfee, whose insight and guidance helped Nils and I decide which direction to take with the project. I would also like to thank those who contributed financially to the project: The College of Physical and Mathematical Sciences at Brigham Young University, who provided funding for my time; and the National Science Foundation, who funded the project through grant number 1205736.

I am grateful for the support of my family as I conducted this research. My parents, Bryan and Angela Jones, instilled in me a passion for learning and a love of science that led me to choose this work. Finally, I am grateful for my wife, Sarah Jones, who let me explain my challenges to her and helped me think through the solutions. Her support has been invaluable.



# Contents

<b>Table of Contents</b>	<b>v</b>
<b>List of Figures</b>	<b>vii</b>
<b>1 Introduction</b>	<b>1</b>
1.1 Wavelength Measurement . . . . .	1
1.2 Determining Sensor Reliability . . . . .	3
1.3 Performance Goals . . . . .	3
1.4 The TCS3414 Color Sensor . . . . .	4
<b>2 Preliminary Considerations</b>	<b>7</b>
2.1 Physical Apparatus . . . . .	7
2.2 Sensor Communication . . . . .	10
2.3 Wavelength Computation Algorithm . . . . .	12
2.4 Intensity . . . . .	13
2.4.1 Bit Noise . . . . .	15
2.5 Temperature Dependence . . . . .	17
2.5.1 Etalon . . . . .	19
<b>3 Results and Conclusions</b>	<b>23</b>
3.1 Precision . . . . .	23
3.1.1 Allan Deviation . . . . .	25
3.2 Accuracy . . . . .	27
3.2.1 Bland-Altman Diagram . . . . .	28
3.3 Future work . . . . .	30
3.4 Conclusion . . . . .	30
<b>Appendix A Minimization Algorithm</b>	<b>33</b>
<b>Bibliography</b>	<b>35</b>
<b>Index</b>	<b>37</b>



# List of Figures

1.1	Color Sensor Diagram . . . . .	5
1.2	TCS3414 Spectral Response Curves . . . . .	5
2.1	Sensor Enclosure . . . . .	8
2.2	Optical Layout . . . . .	9
2.3	Unsanded CS Package Calibration . . . . .	13
2.4	Intensity Fluctuations . . . . .	14
2.5	Error Generated by Bit Noise . . . . .	15
2.6	Temperature Dependence . . . . .	18
2.7	Etalon Diagram . . . . .	19
3.1	Wavelength Measurements Over Time . . . . .	24
3.2	Allan Deviation . . . . .	25
3.3	Unsanded CS Package Calibration . . . . .	27
3.4	Bland-Altman Diagram . . . . .	29



# List of Tables

1.1	Current Wavelength Measurement Methods . . . . .	2
-----	--	---



# Chapter 1

## Introduction

Lasers are common tools in atomic, molecular, and optical physics. Because of their coherence, lasers interact with matter in unique ways. Laser beams serve as diffraction gratings for matter waves, and can cool, trap, and excite atoms. Each of these uses requires the wavelength to be tuned precisely and accurately. For example, the excitation of an atom requires the energy of the photon to match the gap between two energy levels in the atom. Because the energy of the photon is inversely proportional to the wavelength of the laser, we can discuss whether the laser will interact with matter in terms of whether it is tuned to the proper wavelength.

### 1.1 Wavelength Measurement

Because the wavelength determines how light interacts with matter, it is important to know the laser's wavelength. We continue with the example of atomic excitation from the previous paragraph. For a laser to drive an atomic transition in the visible spectrum, a typical resonance transition has a width of a few picometers, which means the wavelength must be known within less than a thousandth of a percent error for the visible spectrum. Measuring the wavelength so accurately has been a problem addressed in recent physics research; John L Hall and Theodor W Hänsch

---

Method	Accuracy	Price (\$)
Frequency Comb	10 attometers	100 000
Interferometer	10 picometers	10 000
Diffraction Grating Spectrometer	1 nanometer	1 000

---

**Table 1.1** The table shows information for a several wavelength measurement tools. The prices and accuracies are representative of the order of magnitude for mid-grade devices, and not the price of a particular model [2].

shared the 2005 Nobel Prize in physics for their work on this subject [1]. Still, the current methods that measure wavelengths to this precision are expensive and use fragile equipment. Table 1.1 gives some information about common wavelength measurement tools.

As consumer electronics develop, one area that receives much attention is digital image quality. Image quality is affected by several factors, including the color of ambient light. Sensors based on photodiode arrays are produced for use in high definition televisions, cameras, and smart phones as a part of image enhancement technology. We will refer to these sensors as color sensors. The sensors provide information about the color of ambient light to the devices, where the information is used for tasks such as color balance adjustment [3]. The demand for high quality images leads to the sensors' mass production, so they cost only a few dollars each.

In an effort to produce the best product possible, color sensor manufacturers design the sensors to the highest specifications they can achieve. The result is that certain models have 16 bits of precision on each of several sets of photodiodes. This indicates that the sensors could potentially distinguish trillions of colors [4], which could make them useful in laser spectroscopy.

In research conducted by Polzer et. al, monochromators were used to show that color sensors can be used to measure the wavelength of light to within 500 pm for much of the visible spectrum [5]. The monochromator in these experiments had a linewidth of 5 nm, so this does not describe the spectrum of a laser well. Additionally, the technology in the sensors used in this research is

based on measuring the depth at which the light is absorbed in the photodiode [5]. We are not aware of research that has been conducted to determine the feasibility of color sensors which use filtered photodiodes instead of penetration depth.

## 1.2 Determining Sensor Reliability

We will use two qualities to describe the performance capabilities of a color sensor. First, we discuss the *precision*. As used in this document, precision refers to the sensor's ability to return the same value over several measurements of the same quantity. This includes both how similar measurements are when made in immediate succession and how similar measurements are when separated in time. This encompasses both the repeatability and stability described by Bolton [6]. If the sensor is able to reproduce the same values, then it can be calibrated such that it will always give the correct wavelength.

However, no sensor is perfectly precise, so the second consideration we will use is *accuracy*. Accuracy refers to the amount by which a measurement may be incorrect [6]. If the sensor is precise, then it can be calibrated to ensure accuracy. Because of the imperfect precision, there will be some error in the calibration. Therefore, we will use the error in measurements made at several wavelengths to quantify the performance of the calibration. In this document, we refer to the performance of this calibration as accuracy.

## 1.3 Performance Goals

Our purpose in testing the performance of the color sensor is to determine if it could be useful for measuring wavelength in a laboratory. If it is able to make measurements accurate to 10 pm or better, the color sensor's performance would be sufficient. This would not be good enough to allow the laser to be directly tuned to an atomic transition. However, it is close enough that a grating

stabilized diode laser could then be scanned to find the appropriate wavelength without mode hopping. Therefore, we set 10 pm precision and accuracy as the benchmark that determines the sensor's laboratory usability. For comparison with the performance of current standard methods, refer back to Table 1.1 on page 2.

## 1.4 The TCS3414 Color Sensor

We will use the TCS3414 Color Sensor manufactured by Texas Advanced Optoelectronic Solutions, Inc. in the experiments that follow. The sensor is manufactured with two different integrated circuit packages or variations, called the CS package and the FN package. This sensor contains an array of photodiodes, which come in four variants: those with a red optical filter, those with a green filter, those with a blue filter, and those with no filter. Figure 1.1 is taken from the data sheet for the TCS3414 and shows the physical layout of the sensors, including the photodiode array [3]. Throughout this thesis, we will call each group a channel, and we label the group with no filter the clear channel. Figure 1.2 shows typical responses for each package, according to the data sheet [3]. After the relative amplitudes of each channel have been measured, the color can be calculated through comparison with previously measured sensor responses to several wavelengths.

The TCS3414's data sheet mentions only two characteristics which seem likely to affect the color sensor's precision. The first is a temperature coefficient, which is 200 ppm/°C; this is listed as applying only to a certain timing control mechanism, and not to optical characteristics. The temperature dependence will be discussed more in Section 2.5. The second is a 16 bit digitizer; this gives 16 bits for each channel, allowing a 48 bit color description, which indicates that the sensor ought to be able to distinguish trillions of colors in the visible spectrum, which has a bandwidth of only 400 nm. This suggested that the sensor could be able to perform much better than is needed for its intended application. This issue will be discussed more in Section 2.4.1. Other limitations

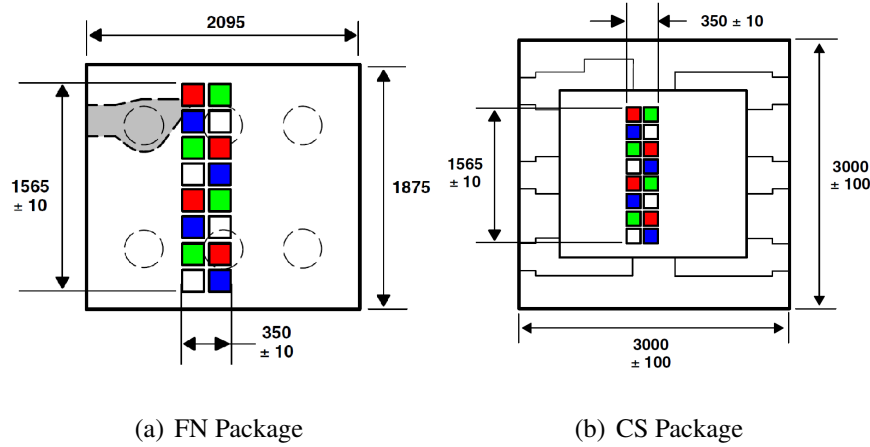


**Figure 1.1** Illustrations of the TCS3414 FN and CS packages. The white squares represent photodiodes with no optical filters. The red, green, and blue squares represent photodiodes with red, green, and blue optical filters respectively, and the dimensions are labeled in micrometers. Figure is reproduced with permission [3].

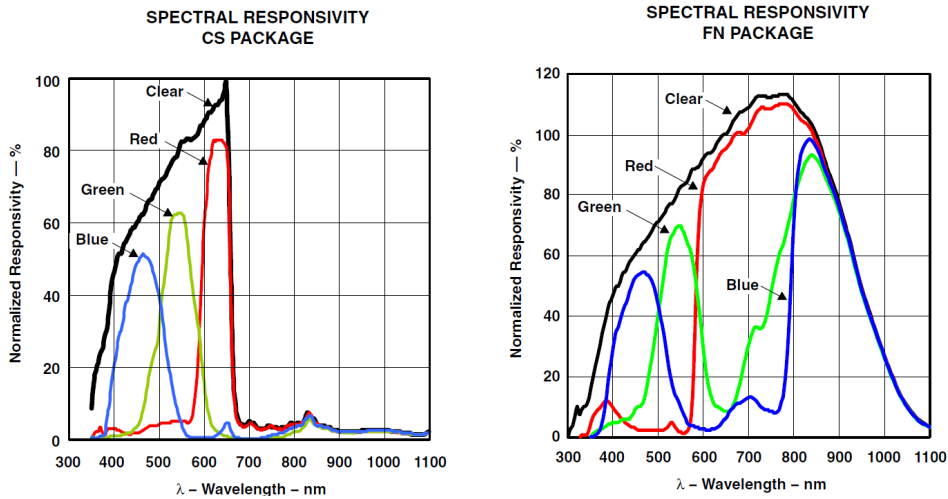


**Figure 1.2** These images, taken from the TCS3414 data sheet, demonstrate typical responses of each of the four channels for both the CS and FN packages. The plot for the CS package is normalized by the clear channel’s value at 655 nm, and the one for the FN package is normalized by the clear channel’s value at 850 nm. Figure is reproduced with permission [3].

are not listed in the data sheet because the sensor was designed to function in broadband light, so it had not been characterized for use with narrow linewidth sources.

A laser's spectrum contains a narrow range of wavelengths and is typically characterized by the peak of the spectrum. While a laser's spectrum has a finite width, it is narrow enough that for the purposes of this work it can be treated as having a single wavelength. We will show that the TCS3414 is able to identify this peak wavelength to a precision of less than 10 pm for time scales less than a day, and is similarly accurate on that time scale. This document will address the method through which the TCS3414 is tested to determine its performance in laser spectroscopy. Chapter 2 will describe a few ideas that must be considered in preparing the sensor for measurements, and Chapter 3 will discuss the sensor's performance.

# Chapter 2

## Preliminary Considerations

Because the sensor was not created for use in laser spectroscopy, there are a few things to consider before we can use it to measure laser wavelength. These include the physical apparatus and the limitations found in the data sheet. This chapter will treat such issues. Sections 2.1, 2.2, and 2.3 give physical and electrical descriptions of the apparatus used to test the sensor. Sections 2.4 and 2.5 describe how the laser's intensity and the sensor's temperature may affect the measurements.

### 2.1 Physical Apparatus

In the tests we conducted, four color sensors were used. Two of these are FN packages, and two are CS packages. This allows us to compare the performances by measuring the same beam simultaneously with all four. We use two of each package to allow tests of the differences in responses for both sanded and unsanded sensors in order to see if the use of an etalon effect increases precision. For more information about etalons, refer to Section 2.5.

In order to measure a laser's wavelength, the sensors must be isolated from other light sources, so we put them in an aluminum case. The dimensions of the box are shown in Figure 2.1. The color sensors are near the center of the PCB, which is shown in green on the left. An optical fiber

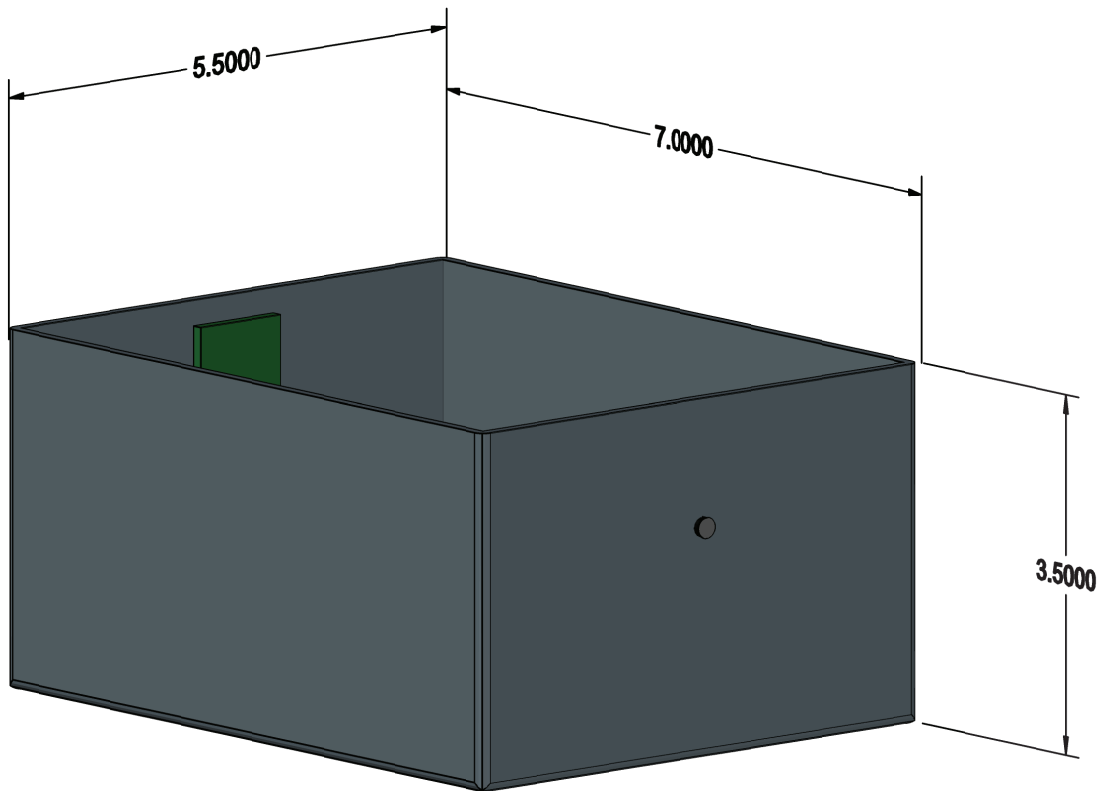


**Figure 2.1** A model of the box containing the four color sensors. The sensors are placed on the PCB shown in green on the left, and the optical fiber is coupled on the right at the small circle. The labeled dimensions are measured in inches.

coupler is located on the side of the case opposite from the sensors. The electrical connections for the sensor come out of a hole behind the PCB which is filled with foam to ensure no light leaks into the box. Inside the box, the sensors measure no light unless the laser is coupled into the case, so we can be confident the sensor will only measure laser light from the optical fiber.

The color sensor's response is dependent on the light's spatial distribution. Because most light is not uniform across a surface, a shift in the sensors position will change the measurement. This is especially problematic for a laser with a profile that has dark spots. For example, if the dark spot initially lies on one of the blue-filtered diodes and then shifts to a red-filtered diode, the relative magnitudes of the light incident on the two channels change greatly. Any consistent beam shape

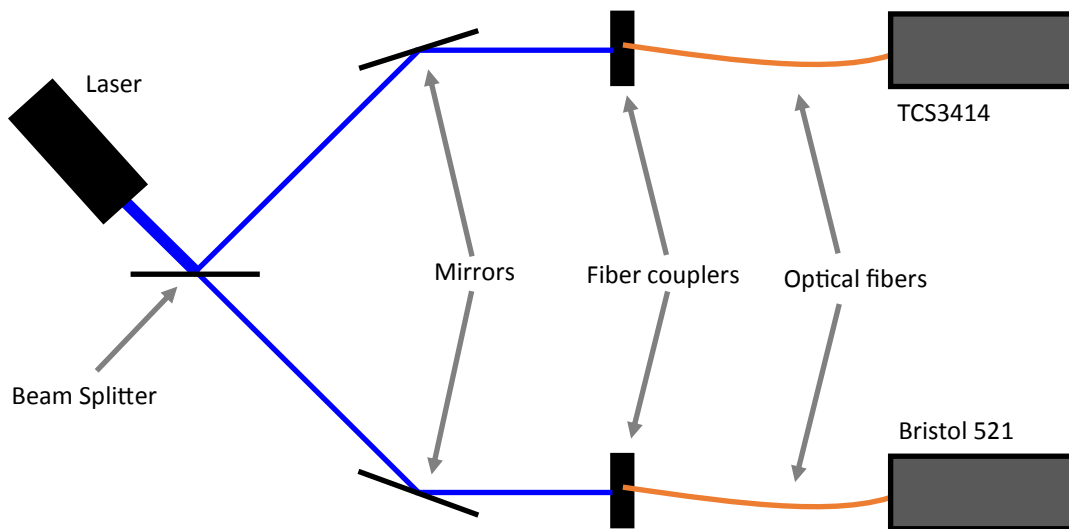


**Figure 2.2** Optical schematic of the experiment. The laser beam is split so that a change in wavelength will be measured on both the set of TCS3414 sensors and the Bristol 521. This allows simultaneous comparison of the color sensors' performance with the commercial meter's performance.

can eliminate the problem, but we chose to use a single mode optical fiber because it gives an easily reproducible beam profile. The fiber we use has a numerical aperture of 0.12 and a core radius of  $1.5 \mu\text{m}$ . For all measurements in this document, other than those related to temperature variation in Section 2.5, we use a 460.8 nm grating stabilized diode laser. Due to the geometry of the fiber and the divergence of the beam, the portion of the beam incident on the PCB has a Gaussian beam width of 1.73 cm. The PCB does not allow fine adjustments to mounting position, so the sensors must remain mounted as well, or their position in the beam will move. Therefore, the sensors must remain in the case between measurements.

We determine the precision and accuracy of the color sensor by comparing it directly to the wavelength measurement obtained by a commercial interferometer, the Bristol 521. We split the laser beam so we can measure the wavelength using the color sensors and the Bristol 521 simultaneously. The optical layout is shown in Figure 2.2.

We use an Arduino Uno microcontroller in this experiment to control the color sensors. The Arduino is configured to communicate with peripherals using a communication protocol called inter-integrated circuit (I<sup>2</sup>C, pronounced "I squared C"), which is described in Section 2.2. The Arduino relays the measurements to a computer using a freeware development environment called Processing through serial communication.

To utilize the entire bit depth of the color sensor, a measurement with a short exposure time is made. Then, Processing computes the amount of time the sensor could be exposed without saturating its analog to digital converter (ADC), and the measurement is repeated with the longer exposure time. Because the TCS3414 has a 16 bit ADC, saturation occurs if one of the channels produces a signal greater than or equal to 65 535. The target value for the clear channel is 55000, which is high enough to utilize the full bit depth of the ADC, but it also leaves room for the laser intensity to fluctuate without saturating the ADC. This second measurement is the one that we use to calculate wavelength.

## 2.2 Sensor Communication

To keep the four sensors' temperature, timing, and incident light uniform, we make measurements with all four sensors simultaneously. This presents the challenge of communicating with them at the same time.

The TCS3414 sensors are configured for use with I<sup>2</sup>C. This protocol connects several devices, called slaves, to a single microcontroller, called the master. Each device is connected to two communication wires: a data line and a clock. The master initiates all communication, either sending commands, or requesting responses through the data line, and the slaves respond with the requested action. Each slave is assigned a unique address, so the master can indicate which device should respond. To send a command, the master transmits the address of the slave it needs to

reach, followed by a code that represents a certain action [7]. The codes for the actions are unique to each device, and can be found in each device's data sheet [3]. If the command is a request for information, the master then listens to the data line, allowing the specified slave to control the data line. The clock is used to synchronize the master and slaves.

Because the TCS3414 sensors were not designed to be used in multiples, each of the sensors has the same address, and there is no way to distinguish the sensors from each other through I<sup>2</sup>C. When the Arduino requests a measurement from the color sensor, all four sensors will attempt to control the data line simultaneously, which causes errors. The solution is to use a set of transistor switches. Rather than connecting the I<sup>2</sup>C data line directly to each sensor, the data line is connected to the collector of an NPN transistor, and the emitter is connected to the sensor. Then, a digital output from the Arduino is connected to the base of the transistor through a 10 k $\Omega$  pull-up resistor. This acts as a digital switch: when the digital line is high, the collector and emitter are connected; when the digital line is low, the collector and emitter are isolated. By connecting a transistor switch to each of the four sensors this way, we are able to control which sensors receive the signals.

If the sensors are not active over the same time period, we will still need to deal with the issue of fluctuating laser intensity, so the sensors must be activated simultaneously. This is possible because the commands that activate and deactivate the sensors' data collection only require an acknowledgement signal from the color sensors. The acknowledgement will be the same signal for each sensor and will occur on the same clock cycle, so this does not introduce error in the operation. Therefore, we can activate all four sensors, allowing them to begin measuring the light, and then deactivate them simultaneously. We only need to isolate the sensors when we try to read measurements from them. After the measurement is completed, we turn on the sensors one at a time and read the measurement, then deactivate that sensor. Each time one of the transistors is activated, a delay is necessary to allow the transistor to fully open before data is transmitted through it. This process effectively allows us to use different I<sup>2</sup>C addresses for each sensor [7].

## 2.3 Wavelength Computation Algorithm

We have developed an algorithm to map the measurements of these four channels to a wavelength. First, we calibrate the sensor. To do this, we measure a sensor's response for a series of wavelengths and divide the red, green, and blue channels by the clear channel. This normalizes the responses, so these ratios depend on the wavelength, but not the intensity of the laser. Then, we generate a least-squares interpolant for the red, green, and blue channels individually. We call these interpolants  $r(\lambda)$ ,  $g(\lambda)$ , and  $b(\lambda)$  respectively, and we use  $\lambda$  to represent the laser's wavelength. Experimentation with the calibration function determined that the measurements from the CS and FN packages are best fit by different fitting functions. The FN package performs well by fitting to a cubic polynomial, shown in Equation 2.1, while the CS package is fit better by the addition of a sinusoid, resulting in Equation 2.2. In these two equations, the  $a_n$  represent fitting parameters, and  $f(\lambda)$  represents the resulting estimate. The fitting function will be different for each channel and each sensor. As a demonstration of what these calibration curves look like, the curves for an unsanded CS package are shown in Figure 2.3.

$$f_{FN}(\lambda) = a_3\lambda^3 + a_2\lambda^2 + a_1\lambda + a_0 \quad (2.1)$$

$$f_{CS}(\lambda) = a_3\lambda^3 + a_2\lambda^2 + a_1\lambda + a_0 + a_4 \sin(a_5\lambda - a_6) \quad (2.2)$$

With this calibration, we are ready to process a measurement. We divide the measurement's red, green, and blue channels by the clear channel, just like we did for the calibration. We call these ratios  $x_r$ ,  $x_g$ , and  $x_b$  for the specific measurement. We calculate the quadrature sum of the percent error of each ratio compared to its corresponding calibration curve. This is shown in Equation 2.3, where  $e(\lambda)$  represents the error as a function of the wavelength  $\lambda$ .

$$e(\lambda) = [1 - r(\lambda)/x_r]^2 + [1 - g(\lambda)/x_g]^2 + [1 - b(\lambda)/x_b]^2 \quad (2.3)$$

Because the values of  $x_r$ ,  $x_g$ , and  $x_b$  are constant for a given measurement, the only variable

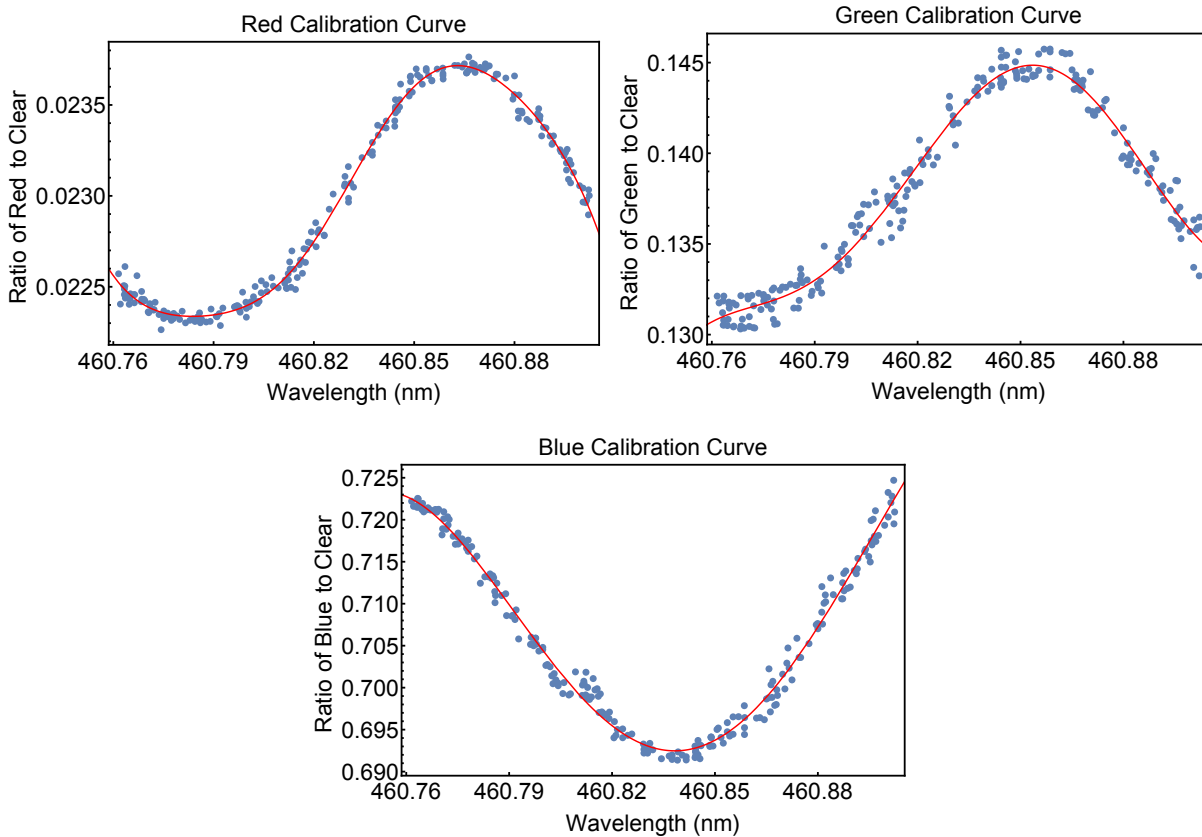


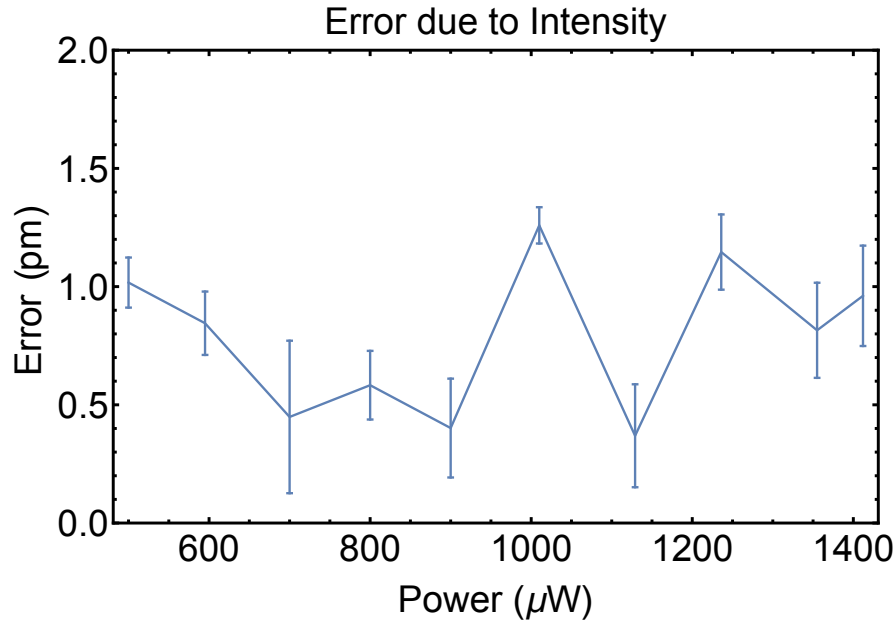
**Figure 2.3** These figures show the three calibration curves for an unsanded CS package. Each point represents a measurement used in creating the calibration, and the curves show the least squares fits that are used as calibration.

in this equation is  $\lambda$ . The value of  $\lambda$  that minimizes  $e(\lambda)$  is the computed wavelength. The minimization algorithm was written in Mathematica, and its code can be found in Appendix A.

## 2.4 Intensity

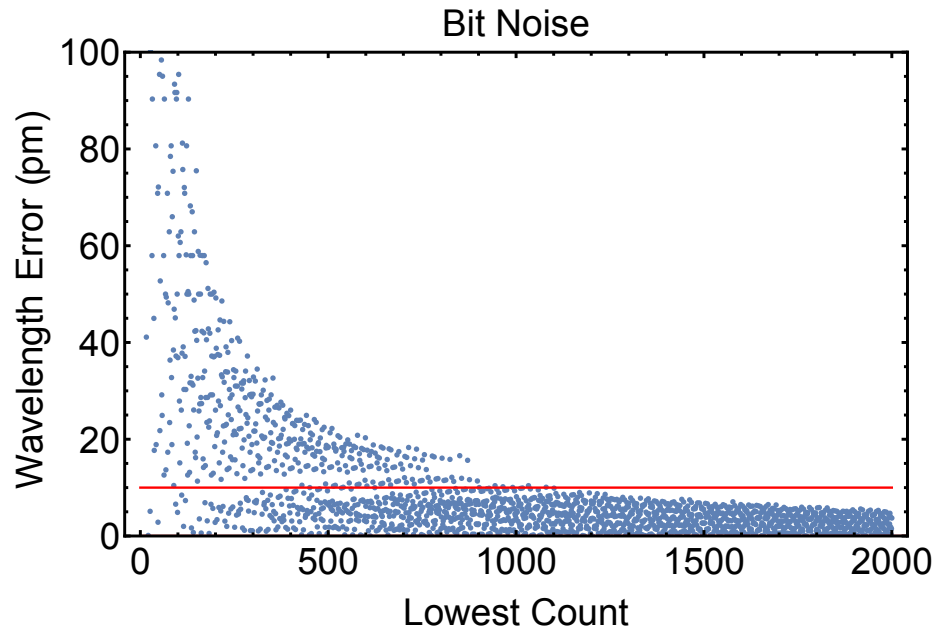
The ratios used for the wavelength calculation in Section 2.3 will only be independent of the laser's intensity if the clear channel and the other channel in the ratio are proportional to the intensity. When this is the case, dividing by the clear channel will normalize for intensity.

Figure 2.4 shows how the computed wavelength changes as the intensity of the light is varied.



**Figure 2.4** The error in wavelength measurement as a function of intensity. We quantify the intensity by measuring the power coupled into the fiber, rather than the intensity incident on the sensor itself. The error is computed by subtracting the calculated value from the wavelength measured by the Bristol 521.

The amount of light is varied using a circular aperture to attenuate the light before it is coupled into the fiber. We quantify the intensity by measuring the power of the beam immediately after the aperture, which assumes that the intensity on each of the sensors will also be proportional to the amount of light coupled into the fiber. While there is slight variation in the error, almost tripling the laser's power has little effect on the error so we conclude that the intensity does not affect the error. The fluctuations in error are also well below the threshold of 10 pm which we set in Section 1.3, meaning that even if the measured wavelength depended on the intensity, it would not be large enough to impact the precision and accuracy enough to cause concern.



**Figure 2.5** The error in computed wavelength due to bit noise. The horizontal axis represents the signal of the lowest value of the four color channel. The vertical axis shows the error in the computed wavelength. The red line marks an error of 10 pm.

### 2.4.1 Bit Noise

Because the measurements come through an ADC, we must be sure that bit noise does not introduce error. Higher intensities, which generate higher measurements on each channel, reduce bit noise because the round-off error is a less significant portion of the signal. However, there is a limitation due to the 16 bit ADC. Each signal must be small enough that it does not saturate the ADC, which means it cannot go above the maximum value. The maximum value for a 16 bit ADC is 65 535. If 65 535 is reached for one channel, the value remains at 65 535 while the values on the other channels can continue to increase. This will cause the ratios to be incorrect. In this section we discuss the error introduced by bit noise as a function of the lowest value of the four channels.

Figure 2.5 demonstrates the error introduced by bit noise. To generate the plot, first we determine the three ratios the calibration expects for light with a 460.8 nm wavelength, which we call

$r_0$ ,  $g_0$ , and  $b_0$ . Using the functions described in Section 2.3, we obtain

$$r_0 = r(460.8\text{nm}), \quad g_0 = g(460.8\text{nm}), \quad \text{and} \quad b_0 = b(460.8\text{nm}).$$

Then, we scale and round the numbers such that

$$r = \lceil\lceil nr_0 \rceil\rceil, \quad g = \lceil\lceil ng_0 \rceil\rceil, \quad \text{and} \quad b = \lceil\lceil nb_0 \rceil\rceil$$

for a broad range of  $n$ , where  $\lceil\lceil x \rceil\rceil$  represents  $x$  rounded to the nearest integer. The clear channel will have magnitude  $n$ , because the ratio of clear to itself is always one. These ratios can then be normalized by division by  $n$ , which results in

$$x_r = \frac{\lceil\lceil nr_0 \rceil\rceil}{n}, \quad x_g = \frac{\lceil\lceil ng_0 \rceil\rceil}{n}, \quad \text{and} \quad x_b = \frac{\lceil\lceil nb_0 \rceil\rceil}{n}. \quad (2.4)$$

We then calculate the wavelength using these  $x_r$ ,  $x_g$ , and  $x_b$  and determine the error  $E$ . For 460.8 nm, red is the lowest channel, so  $|E|$  is plotted against  $x_r$  in Figure 2.5. This process simulates bit noise and allows us to examine the error which bit noise introduces.

As the figure shows, we can be confident that the bit noise will not cause the sensor to have an error greater than 10 pm as long as the lowest channel is more than about 1000. However, according to the curves of Figure 1.2 on page 5, there is a small range of wavelengths around 550-560 nm for which the lowest channel cannot reach 1000 unless the clear channel saturates [3]. To overcome this limitation, we use a normalization technique to increase the bit depth of the sensor. To describe this approach, we use an example. For 460.8 nm light, the weakest channel is the red, so it is most likely to underutilize the full range of the ADC. To simulate a greater bit depth, we first make a normal measurement. We then maintain the clear and blue channels from that measurement, because they have the highest values. We call them  $c_1$  and  $b_1$  respectively. We will also discuss  $g_1$ , the green channel from this measurement. Then, we make a second measurement, allowing the clear channel to saturate, but not the blue channel. From this, we maintain the blue and green channels, which we call  $b_2$  and  $g_2$ . A third measurement is made, allowing the clear and

blue to saturate, but not the green or red. The green and red values,  $g_3$  and  $r_3$ , are kept. The second and third measurement pairs are then multiplied by normalization constants  $a_2$  and  $a_3$ , so the three measurements are

$$[c_1, b_1], \quad [a_2 b_2, a_2 g_2], \quad \text{and} \quad [a_3 g_3, a_3 r_3].$$

Now, we have a set of measurements which can be used to determine  $a_2$  and  $a_3$ . The value of  $a_2$  should be chosen so that  $a_2 b_2 = b_1$ , or  $a_2 = b_1/b_2$ . Because  $b_2$  was nearer to saturation than  $b_1$ ,  $a_2$  is less than one, and because  $b_2$  and  $g_2$  are both proportional to the intensity of the laser and the exposure time, choosing  $a_2$  as described above will scale  $g_2$  to be near  $g_1$ . However, because  $g_2$  is larger than  $g_1$ , it will utilize more of the ADC, and will be a more exact measurement. We use a similar process to scale  $r_3$  in a similar way. The end result is a set of four values,

$$[c_1, b_1, \frac{b_1}{b_2} g_2, \frac{g_2}{g_3} r_3],$$

that represent the clear, blue, green, and red channels respectively. These can then be used to compute the wavelength.

Therefore, the only limitation caused by intensity is that the signal of the weakest channel must be larger than 1000, which can be accomplished simply by increasing the sensor's exposure time. If this condition is met, this does not guarantee that overall precision will be less than 10 pm, but it does ensure that bit noise and intensity will not be the cause of an error that large. If one of the signals drops below that limit, then the error due to the bit noise begins to have an effect. The intensity, however, does not directly affect the wavelength measurement.

## 2.5 Temperature Dependence

One of the limitations listed in the data sheet for the TCS3414 is a temperature coefficient of 200 ppm/°C [3]. This represents a small deviation in measurements for small temperature changes.

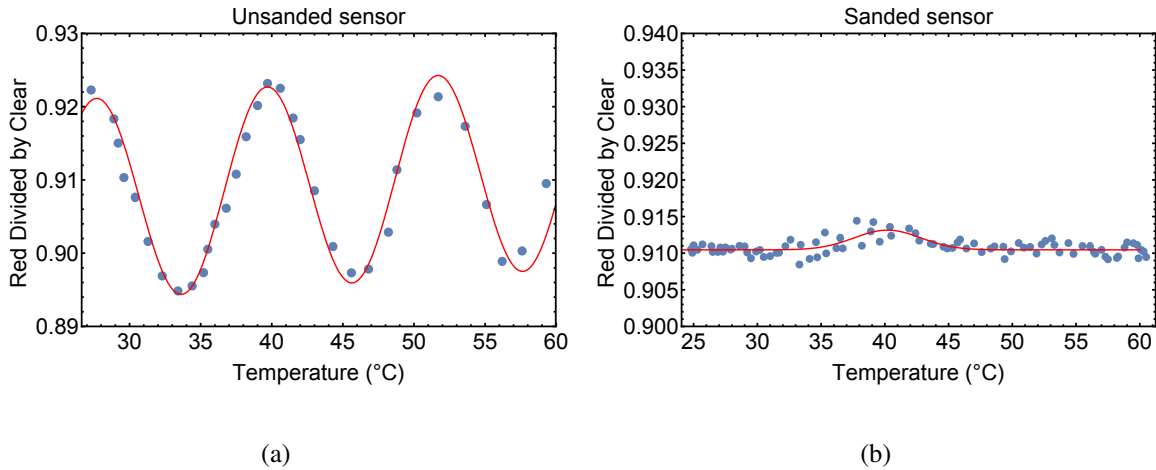


**Figure 2.6** Etalon in the FN package. This shows how the ratio of the red channel to the clear channel changes as the temperature is varied for 2.6(a) an unsanded sensor and 2.6(b) a sanded sensor.

However, this coefficient only refers to measurements made when the integration time is controlled by one of the integrated circuit's pins, which is called the sync pin, so it is probably a limitation of the timing electronics or interrupt system rather than an optical limitation. We do not operate with the sync pin: we use external timing based on the Arduino clock, so we made preliminary measurements to ensure that there is no temperature dependence when using external timing. The laser used for these measurements was a 632.8 nm Helium-Neon laser.

What we found is surprising. Figure 2.6(a) plots the ratio of the red channel to the clear channel from the unsanded FN package against the sensor's temperature, and its dependence is sinusoidal. The amplitude of the sinusoid gives fluctuations much larger than 200 ppm/°C, but this effect is almost negligible in the CS package. Because there are thin films in these sensors (e.g., plastic coatings, epoxies, and the optical filters), we explore whether this could be due to an etalon.

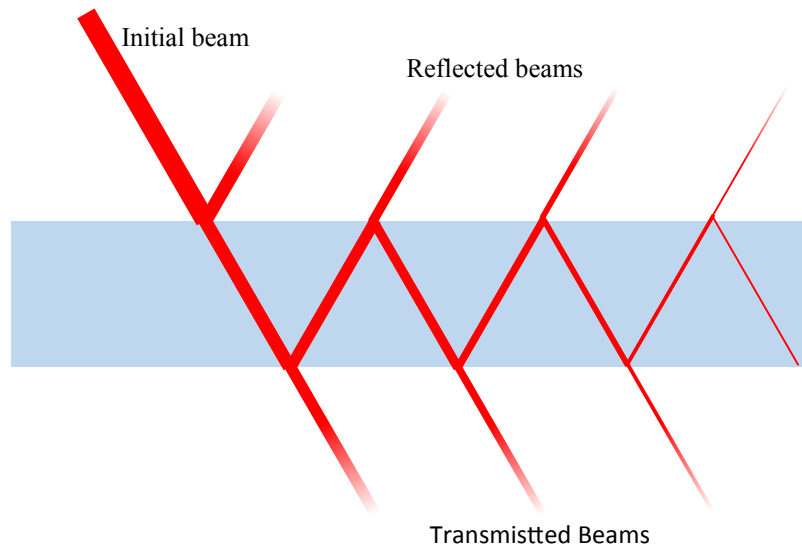


**Figure 2.7** The reflections that cause an etalon. The series of dark and bright fringes is caused by interference of these beams.

### 2.5.1 Etalon

An etalon is a device which causes thin film interference and is the core component of Fabry-Perot interferometers. When there is a change in the index of refraction, light reflects. The reflections shown in Figure 2.7 demonstrate how light will reflect repeatedly on the surfaces of a thin film. If the light approaches at or near normal incidence, the beams will line up with each other and interfere. Because the transmitted beams further to the right have traveled further inside the film, they will be out of phase with the leftmost transmitted beam. The phase difference depends on the thickness, as does the resulting interference pattern [8]. The phase also depends on the wavelength, because traveling the same distance with a shorter wavelength would give a greater phase change.

A phase shift of  $2\pi$  is the same as having no phase shift. Therefore, an etalon will cause the amount of transmitted light to vary periodically with the thickness of the film. It appears that one or more of the sensor's thin films acts as an etalon.

If the sensor does have a film acting as an etalon, the amount of light transmitted to the pho-

todiodes will depend on the wavelength of the light and the thickness of the film. However, the observed periodic behavior appeared as the temperature varied. The connection between temperature and the etalon is thermal expansion. As the sensor's temperature increases, the thicknesses of the films in the sensor increase as well. Therefore, thermal expansion allows the sensor to act as an etalon.

To eliminate the etalon, we alter the sensor's optical properties. Using sandpaper, we remove the fine finish of the sensor. This does not stop the reflection of the light, but it does randomize the direction of those reflections. The randomized angles will cause different parts of the reflected beams to interfere differently with each other in a less coherent way, which will "wash out" the etalon's effect. Figure 2.6(b) on page 18 shows the temperature measurement for a sanded sensor. The periodic behavior has been greatly reduced, so we conclude that it was indeed an etalon.

The etalon is influenced by many factors, including the indices of refraction, thicknesses, and the order of compounds. The reason the etalon does not appear in the CS package is likely due to the differences in sensor geometry — including dimensions — and manufacturing.

The etalon is an example of one of the effects that was not considered in the design of the sensor. The sensor was made for use with broad spectra of light. In broadband light, one given wavelength may have destructive interference while a nearby wavelength has constructive interference. The two nearby wavelengths cause opposite responses that are similar enough in magnitude to leave the total transmission largely unchanged. This allows the sensor to function with broadband light without regard to the temperature. However, for narrow linewidth light, the temperature needs to be controlled. To do this, we mounted a thermo-electric cooler and a thermister to the back of the PCB. These are connected to a PID controller, and the sensor's temperature is maintained constant.

While we expect the temperature dependence in the etalon to decrease accuracy and precision, an etalon's effects are also dependent on wavelength. We explored whether the etalon could improve precision by giving more variation to the calibration curves by comparing results of sanded

and unsanded sensors. Note, however, that the amplitude of the fluctuations due to the etalon is small compared to the total amplitude of the response, so it would only have minor effects. These results are presented in Chapter 3.



# Chapter 3

## Results and Conclusions

This chapter addresses the precision and accuracy of the TCS3414 in Sections 3.1 and 3.2 respectively, and each is accompanied by its own metric. This is followed by a brief discussion of other work that could build upon that presented here (Section 3.3) and conclusions (Section 3.4). Please notice that the CS color sensor performs similarly well to the Bristol 521 in these tests.

### 3.1 Precision

Without sufficient precision, calibration cannot provide a good description of how the sensor behaves, so we address the precision before the accuracy. This section addresses the precision for time periods on the order of a day. To quantify the sensor's precision, we need the wavelength of the laser we use to be constant. Otherwise, any discrepancies between two measurements could be due to drift in the sensor or changes in the wavelength. We achieve a constant wavelength by locking the laser to an atomic transition of Strontium using saturated absorption spectroscopy. This guarantees that any drift we see in measurements is a drift in the sensor and not in the wavelength.

After locking the laser, we took continuous wavelength measurements over ten days using five devices: an unsanded FN package, a sanded FN package, an unsanded CS package, a sanded CS

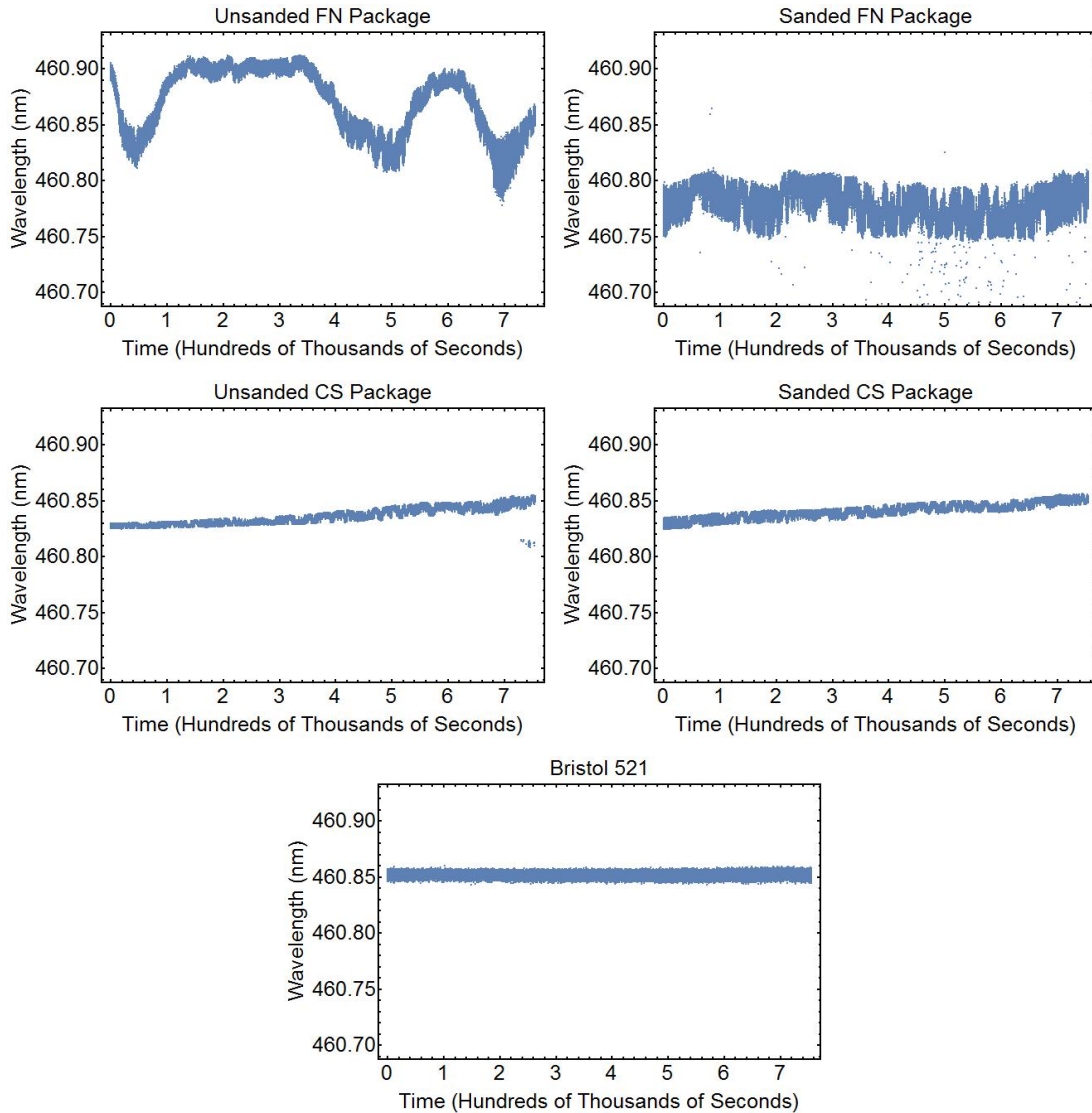


**Figure 3.1** The measurements from the five devices over a period of ten days. Measurements for each device were made simultaneously using a laser which was locked to Strontium’s atomic transition near 460.8 nm.

package, and a Bristol 521. The Bristol 521 is a standard to compare with the deviations of the color sensors. These measurements are shown in Figure 3.1. No device is perfectly precise, so we expect some spread in the measurements, but the general shape will not change with time for an instrument with good long term precision. The device that accomplishes this best is the Bristol 521, and other than the upwards drift, the CS package is comparable to the Bristol 521. We will

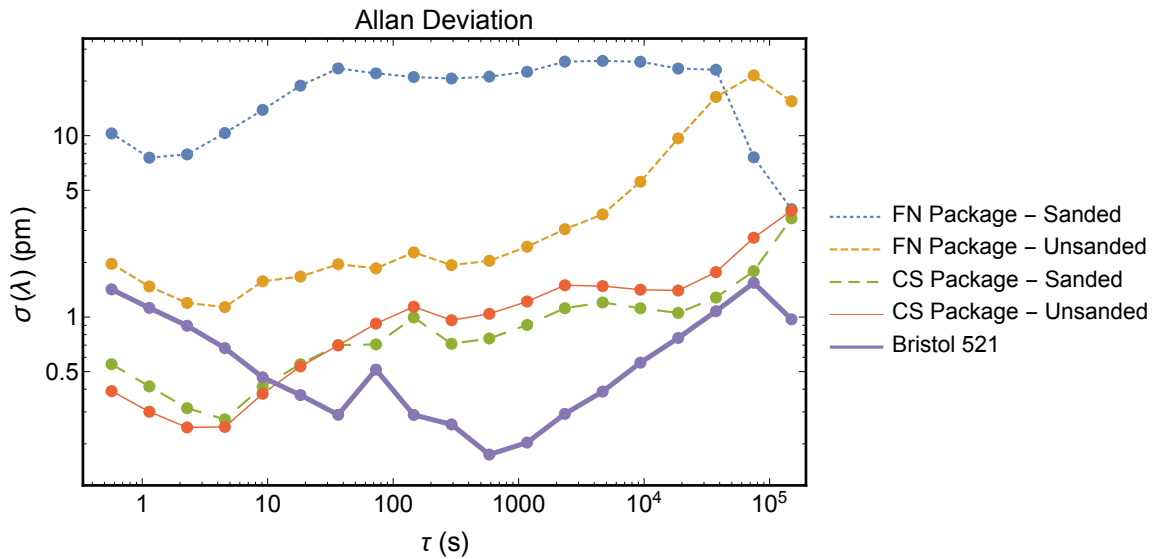


**Figure 3.2** The Allan deviation of the four color sensors and the Bristol 521. Measurements were taken over a period of 10 days.

now quantify the precision of these measurements using the Allan deviation.

### 3.1.1 Allan Deviation

The Allan deviation is a way to describe how closely correlated measurements at one time are to measurements at another. Let  $\tau$  be a time interval. Let  $N(\tau)$  be the number of measurement pairs for which one of the measurements in the pair was made at a time  $\tau$  after the other and  $\Delta\lambda_n$  be the difference of the  $n^{\text{th}}$  measurement pair. The Allan deviation calculates the average error between those  $N$  pairs. If the error is small for short  $\tau$ , it means that measurements are precise over short time periods, and if the error is small for large  $\tau$ , then it means that the measurements are precise over long time periods. Therefore, it is a good measurement of the precision of the color sensor. Equation 3.1 shows the formula for the Allan deviation [9].

$$\sigma_{\lambda}(\tau) = \sqrt{\frac{1}{2N(\tau)} \sum_{n=1}^{N(\tau)} \Delta\lambda_n^2} \quad (3.1)$$

Figure 3.2 shows the Allan deviation for our four color sensors (FN and CS packages, with

sanded and unsanded variations of each) and the Bristol 521 using the data shown in Figure 3.1. The largest value of  $\tau$  in this figure is on the order of one day. This is less than the ten days of data which are shown in Figure 3.1 because it allows us to have a significant number of measurements to average over. The FN package has the poorest performance. It is important to note, however, that the FN package improved by roughly an order of magnitude for shorter time scales by being left unsanded. This indicates that the etalon contributes to the sensor's ability to distinguish wavelengths. As time goes on, the etalon becomes less useful as the sensor drifts, because the etalon represents only a small percentage of the response (see Section 2.5.1). This also implies that for the FN package, controlling the temperature is crucial, because fluctuating temperature will disallow the etalon's use in this way. For the CS package, on the other hand, there is no significant difference between the sanded and unsanded variations. This is consistent with our observation in Chapter 2.5.1 that there was no etalon in the CS package. Additionally, the CS package is comparable to the Bristol 521. The interferometer does perform much better for  $\tau$  near 1000 s, but otherwise they are similar.

As the length of time increases, there is a general upward trend for the sensors. This is expected because all sensors will drift to some extent. The Allan deviation is only shown here for time scales up to about a day. To verify that there is little drift over a time period closer to the length of time for which a wavelength meter would be used in a laboratory, the Allan deviation ought to be calculated for time scales of months and years. While time has not been sufficient to allow this in my research, these measurements do show that for short time scales, the CS package performs with a precision similar to that of the Bristol 521. This does not guarantee that the color sensor is stable over large time scales, but it is a good indicator that it could be. At the very least, it is likely comparable to the Bristol 521 over those time scales. Additionally, the CS package remains below 10 pm, which is repeatable enough to allow the goal of 10 pm accuracy.

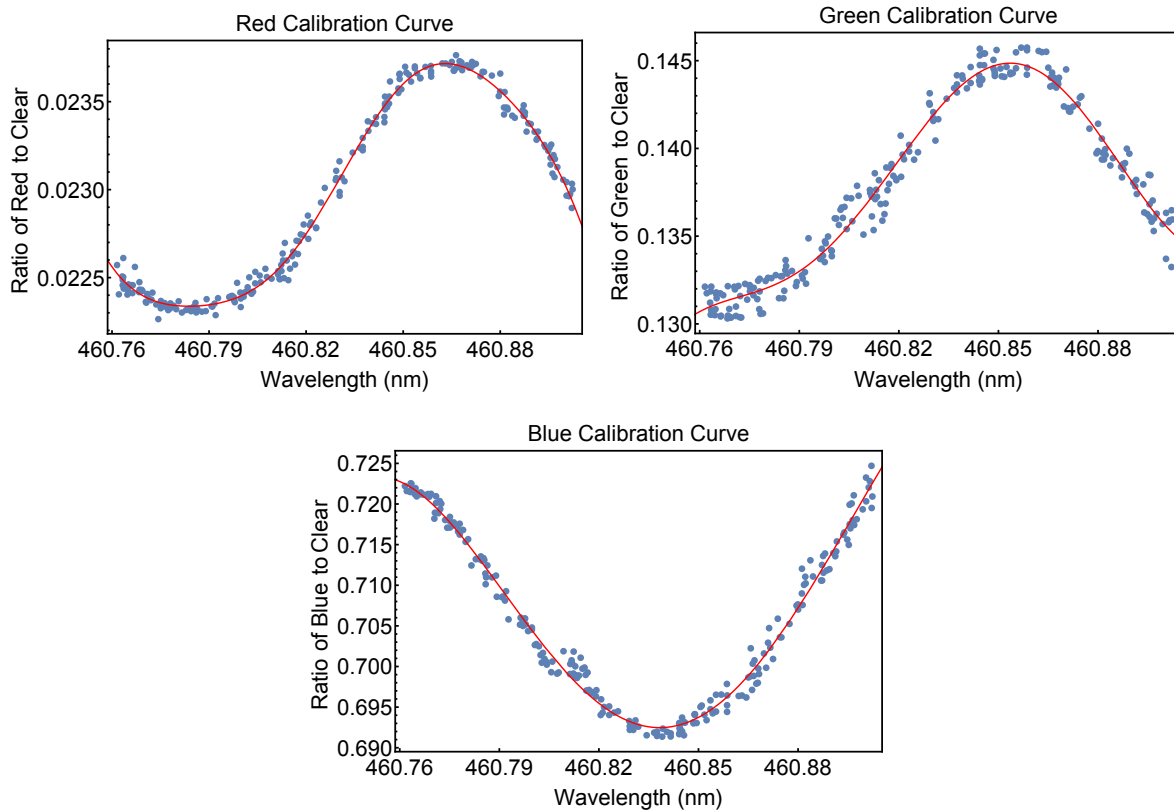


**Figure 3.3** A reproduction of Figure 2.3, shown here for convenience. These figures show the three calibration curves for an unsanded CS package. Each point represents a measurement used in creating the calibration, and the curves show the least squares fit that are used as calibration.

## 3.2 Accuracy

Because we have shown that the sensor is precise to less than 10 pm, we can proceed with the accuracy discussion. Recall from Section 1.2 that we use the term accuracy in reference to the performance of the calibration over a range of wavelengths. Calibration curves for the unsanded CS package are shown in Figure 3.3. Each point is a measurement used in creating the calibration, and the curves are the least squares fit, as described in Section 2.3. Because the calibration curve is an estimate only, there will be some error in the computed wavelength. Our discussion of accuracy will help us quantify that error. In this section, we make measurements of the laser wavelength for

99 wavelengths within these calibration curves. Because we cannot lock the laser for each of the wavelengths in this range, we must use a different metric to determine the accuracy. We will use a Bland-Altman diagram.

### 3.2.1 Bland-Altman Diagram

A Bland-Altman diagram is a way of demonstrating the correlation between two measurements of the same quantity and is often used to compare two different sensors [10] [11]. Let  $\lambda_a$  represent the wavelength measured by one of our color sensors and  $\lambda_b$  represent the wavelength measured by the Bristol 521. The Bland-Altman diagram is created by plotting their differences against their average. That is, for a measurement pair  $(\lambda_a, \lambda_b)$ , an ordered pair called  $M$  is generated, as shown in Equation 3.2. A plot of all  $M$  is called a Bland-Altman diagram.

$$M = \left( \frac{\lambda_b + \lambda_a}{2}, \lambda_b - \lambda_a \right) \quad (3.2)$$

Figure 3.4 shows a Bland-Altman diagram for the unsanded CS and FN packages. We show only the unsanded sensors for this figure because the unsanded FN package performed better than the sanded FN package. There was no clear result as to whether the CS package performed better sanded or unsanded, but using the unsanded sensor does not negatively impact the precision, but using an unmodified CS package is convenient for comparison. Each plot includes more than 1500 measurements. Only two of those lie outside of the 10 pm benchmark for the CS package. Therefore, for the majority of measurements, the CS package is accurate to within 10 pm. The average error for the CS package measurements shown is 3.16 pm. Figure 3.4(b) shows that the spread for an FN package is about ten times as large; its average deviation is 22.5 pm. Therefore, the CS package is able to be calibrated much more accurately.

There is also an interesting pattern in the plot of the FN package. While the CS package gives a random spread around an error of zero, there are three distinct units in the FN diagram. This

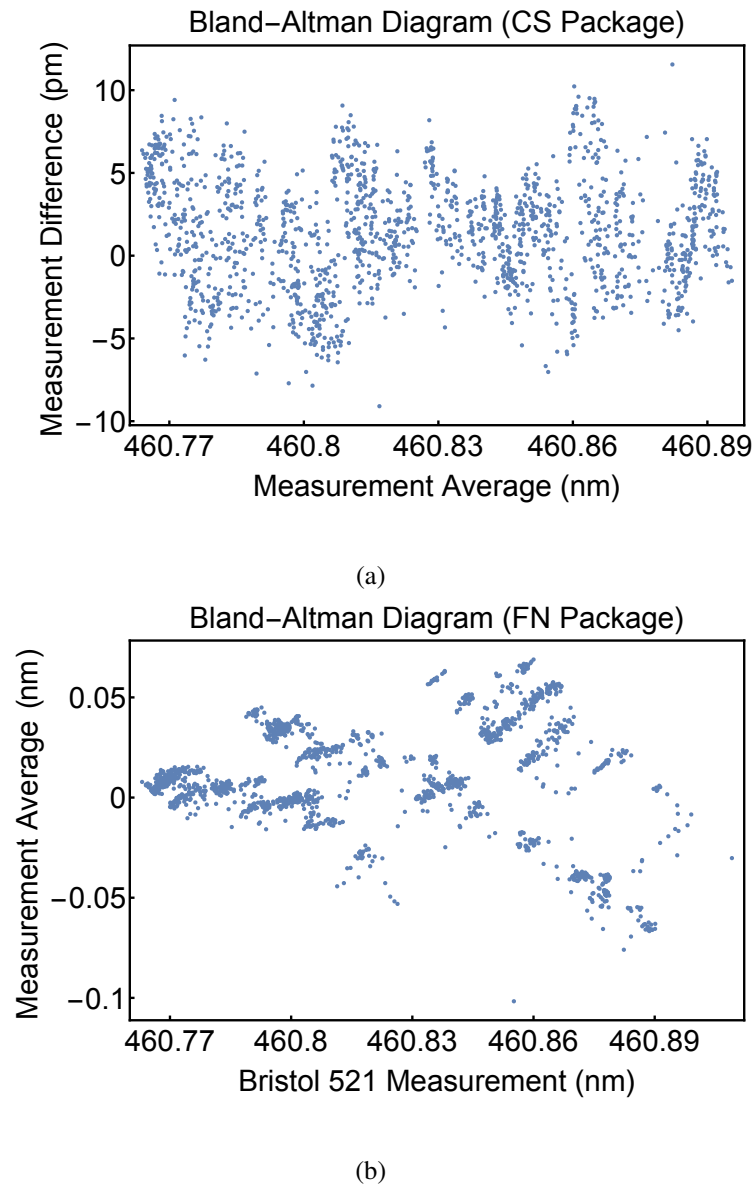


**Figure 3.4** A Bland-Altman Diagram of the performance of an unsanded CS package of the TCS3414 Color Sensor and the Bristol 521.

occurs because the calibration for the FN package is much flatter than the calibration for the CS package, which creates multiple local minima. If the calibration curves were steeper, they would be able to tell which of these minima is the actual wavelength, and this error would be reduced.

### 3.3 Future work

Thus far, we have discussed the capabilities of the TCS3414 CS and FN packages, which were not designed for use in laser spectroscopy. This mostly limits us to external modifications and algorithmic strategy. However, it is possible that the internal workings of the sensor could be modified to improve them. Further work could be completed to improve a sensor such as these. For example, the integrated circuit could be constructed using different colored filters or with more channels. Such design approaches from an engineering firm could increase the performance of the device.

Additionally, the sensor was tested over a limited range of wavelengths, only about 0.15 nm. Testing in other wavelength ranges, or over the entire optical spectrum using a monochromator, is necessary to give information about the response in other regions. The timescale must be lengthened as well: the Allan deviation presented in Section 3.1 only describes the precision for periods on the order of a day. Because the wavelength meters are tools which are used for timescales on the order of years, the sensor's precision over longer time scales must be characterized.

### 3.4 Conclusion

In Chapter 1, we set a performance goal of 10 pm. We aimed to have the accuracy below this value, but the precision affects the accuracy, so the precision must be below this value as well. Otherwise, the accuracy could not be that good. Recall that we chose 10 pm because this is accurate enough that a laser can then be scanned to find an atomic transition without mode hopping, and that this is comparable to the performance of a mid-grade interferometer.

The two metrics we use to determine how well the wavelength can be measured using a color sensor are the Allan deviation and a Bland-Altman diagram. For the unsanded CS package, The Allan deviation shows that over short time scales, a precision of a few picometers can be achieved,

and for a time period of a day, it is still precise to 3.86 pm (see Figure 3.2). Additionally, the Bland-Altman diagrams in Figure 3.4 show that the calibration is able to measure wavelengths over a range of 150 pm to an accuracy of 3.16 pm as well, indicating that the sensor is also capable of distinguishing wavelengths. Therefore, overall, the sensor is accurate to within 10 pm for time scales on the order of a day. Its performance over this time scale is comparable to the Bristol 521, which uses interferometry to determine the wavelength. The FN package, on the other hand, does not perform well enough to reach this goal. Its Allan deviation shows that it will vary by 21.5 pm throughout a day. Because it is so much less precise than the CS package, the FN package cannot be calibrated as well. This can be seen in the wide spread of wavelengths of its Bland-Altman diagram (see Figure 3.4(b)), which gives an average error of 22.5 pm. The CS package is more precise and more accurate by a factor of ten.

While this does not guarantee that color sensors are useful in laser spectroscopy, it is encouraging. This comparison has only been determined for time scales on the order of a day. For longer time scales, performance is as of yet unknown, but the sensor has the potential to perform on par with commercial interferometers.



# Appendix A

## Minimization Algorithm

The following code is written in Mathematica. It creates a function `findλ[DATA]` that takes a variable `DATA` as input, where `DATA` is a list with four elements: the signals of the clear, red, green, and blue channels for one measurement. The value returned is the wavelength which minimizes the error between the signals measured and the calibration curve.

```
error[x_, DATA_] := 2(1 - redf[x]/(DATA[[2]]/DATA[[1]]))^2 + 0.5 (1 - greenf[
  x]/(DATA[[3]]/DATA[[1]]))^2 + 2 (1 - bluef[x]/(DATA[[4]]/DATA[[1]]))^2
findλ[DATA_] := Module[{z, derivative, ans, maxL, answerIndex, smallest,
  maxAllowable, probablyNot, step, possibleSolution},
  (*Each minimization algorithm is accurate at different times, so we use both
  NMinimize and FindMinimum. Then, we manually compare to find the lowest
  value*)
  ans = {NMinimize[error[x, DATA], x, AccuracyGoal -> 20, PrecisionGoal -> 20,
    WorkingPrecision -> 25][[2, 1, 2]]} // Quiet;
  (*We have not calibrated beyond 461 nm, so we do not allow wavelengths at
  that value*)
  maxAllowable = 461;
  (*If there is a value with a negative second derivative, it is likely a
  local max, so we disregard it*)
```

```
probablyNot = {};  
  
(*Find Minimum requires estimates for solution seeking. We loop through  
multiple guesses to find all local minima*)  
step = .04;  
Do[possibleSolution = FindMinimum[error[x, DATA], {x, estimate}, Method -> "  
ConjugateGradient", WorkingPrecision -> 20][[2, 1, 2]] // Quiet;  
If[(D[derivative, x] /. x -> possibleSolution) >= 0,  
  If[possibleSolution < maxAllowable,  
    AppendTo[ans, possibleSolution],  
    AppendTo[probablyNot, possibleSolution]]];  
  , {estimate, 460.74, 460.95, step}];  
  
(*The smallest error*)  
smallest = Min[error[ans, DATA]];  
Do[If[error[ans[[j]], DATA] == smallest, answerIndex = j;  
  Break], {j, 1, Length[ans]}];  
ans[[answerIndex]]  
]
```

# Bibliography

- [1] John L. Hall, “Defining and Measuring Optical Frequencies: The Optical Clock Opportunity - and More,” [http://www.nobelprize.org/nobel\\_prizes/physics/laureates/2005/hall-lecture.pdf](http://www.nobelprize.org/nobel_prizes/physics/laureates/2005/hall-lecture.pdf) (Accessed 20 April 2015).
- [2] D. Durfee, Private Communication, 2013.
- [3] Texas Advanced Optoelectronic Solutions, “TCS3404, TCS3414 Digital Color Sensors,” <http://www.ams.com/eng/content/download/250257/975989/142696> (Accessed 26 July 2012).
- [4] D. Allen, Private Communication, 2014.
- [5] A. Polzer, W. Gaberl, and H. Zimmermann, “Wavelength detection with integrated filter-less BiCMOS RGB sensor,” *Electronics Letters* **47**, 614–615 (2011).
- [6] W. Bolton, *Mechatronics: a Multidisciplinary Approach* (Pearson Education, 2008).
- [7] D. Eisenreich and B. DeMuth, *Designing Embedded Internet Devices* (Newnes, 2003).
- [8] J. Peatross and M. Ware, *Physics of light and optics* (Brigham Young University, Department of Physics, 2011).
- [9] J. A. Barnes and D. W. Allan, “Variances based on data with dead time between the measurements,” Technical report, DTIC Document (1987) .

- [10] J. M. Bland and D. G. Altman, “Comparing methods of measurement: why plotting difference against standard method is misleading,” *The Lancet* **346**, 1085–1087 (1995).
- [11] A. Brennan, J. Zhang, K. Deluzio, and Q. Li, “Quantification of inertial sensor-based 3D joint angle measurement accuracy using an instrumented gimbal,” *Gait & posture* **34**, 320–323 (2011).

# Index

I<sup>2</sup>C, 10

abstract, ii

accuracy, 3, 27, 28, 31

algorithm, 12, 33

Allan deviation, 25

analog to digital converter (ADC), 10, 15

bit noise, 15

Bland-Altman diagram, 28

etalon, 18, 19, 21

intensity, 13

performance goals, 3, 31

physical apparatus, 7

precision, 3, 23, 25, 26, 31

TCS3414, 4

temperature, 17, 21

transistor switch, 11